RSC Advances

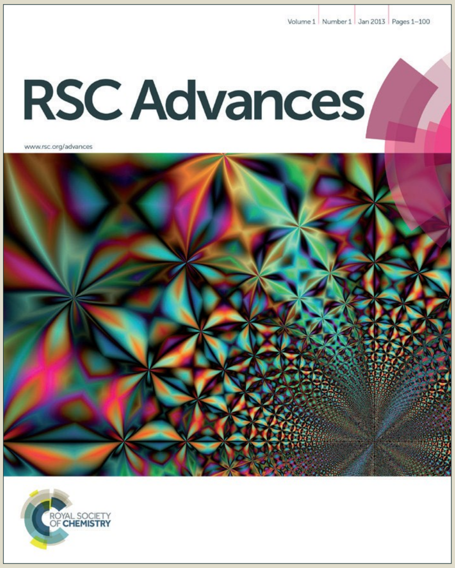

ROYAL SOCIETY OF CHEMISTRY

www.rsc.org/advances

A new and accurate expression for radial distribution function of the confined Lennard-Jones fluid in carbon nanotube

Mohsen Abbaspour,* Hamed Akbarzadeh, Mousarreza Abroodi
Department of Chemistry, Hakim Sabzevari University, Sabzevar, Iran

Abstract

Molecular dynamics (MD) simulations have been performed to generate the radial distribution functions (RDFs) of confined Lennard-Jones (LJ) fluid into (33,0) carbon nanotube (CNT) from room temperature to 600 K. Then, we have fitted the obtained RDF values to a new analytical expression in a good accordance with the simulated values. The new RDF expression predicts the configurational energy and the radial and axial pressures of the LJ fluid with an uncertainty that is comparable to that obtained directly from the MD simulations.

---

* Corresponding author. Tel.: +985144013322
E-mail Address: m.abbaspour@hsu.ac.ir; mohsenabbaspour@yahoo.com

1. Introduction

Reduction of the size of a substance to the nanometer scale endows it with the properties and behavior that are different from those of the bulk material.[1] The interaction with the walls that confine a sample in a small volume further alters the properties, behavior, and structure of the material. For example, gas and liquid inside a carbon nanotube (CNT) has a remarkable change because of the nanoscale confinement for the molecular motions.[2,3] These unconventional phenomena provide a challenge for the development and application of the fluids at nanoscale.[4] Among the different properties of the fluids which may changes in the nanoconfinement state, the radial distribution function (RDF) is of great importance which has been the subject of some recent investigations.[5,6] The RDF is the best characteristic of the nature of substances, specially liquids, and its knowledge could reveal the peculiarities of fluids and fluid mixtures.[7] It acts as a bridge for relating macroscopic thermodynamic properties to interparticle interactions of substances.[8] For a normal (non-confined) fluid, knowledge of the RDF is very important because of the following reasons; First, the knowledge of the RDF is sufficient to calculate the thermodynamic properties such as the pressure and internal energy. Second, the RDF allows us to calculate direct correlation function integrals which are the basis of the fluctuation theory of mixtures. Third, the RDF is the best characteristic of the nature of fluids.[7-11] For these reasons, there are many investigations about the RDF of the fluids and fluid mixtures. For example, Matteoli and Mansoori[12] presented a simple expression for the RDF of a LJ fluid using 21 parameters at different values of temperature and density. Their values of the reduced pressure and internal energy calculated by numerical integration of the completely parametrized RDF equation, have been compared fairly with literature MD simulation results. Morsali et al.[8] presented an accurate expression for the RDF of the LJ fluid with total of 65 constants as a continuous function of reduced interparticle distance, temperature, and density. Their expression predicted the pressure and the internal energy of the LJ fluid with an uncertainty which was better than the expression of Matteoli and mansoori.[12] Abbaspour and Keyvanloo[13] determined an analytical expression for RDF of the Hartree-Focked Dispersion (HFD)-like fluid. They also calculated the pressure, internal energy, and infinite-frequency shear modulus of the HFD-like fluid using statistical mechanical formulas. They also investigated many-body and quantum corrections for the RDF of the HFD-like fluid. Abbaspour and Jorabchi[14] developed the RDF expression of Abbaspour and Keyvanloo[13] for the HFD-like fluid as a continuous function of reduced interparticle distance, temperature, and density. They also calculated the shear viscosity, self-diffusion coefficient, and thermal conductivity of the HFD-like fluid using the proposed RDF equation and the many-body and quantum corrections.

The RDF of the confined fluids and nanoparticles into the CNTs or slit pores has been also subject of some of the works in recent years.[5,6,15] For example, Das and Singh[5] calculated radial distribution function to analyze the structure and phase for each layer of confined LJ system into slit pores. To gain insights into the local structure of a confined ionic liquid (IL) in silica nanopores, Ori et al.[15] calculated the pair correlation functions between the cation or anion of the IL and atoms of the silica surfaces and between the cation and anion of the IL. In order to better understand the melting and freezing of confined copper nanoclusters into CNTs, Akbarzadeh et al.[6] employed the Cu-CNT RDFs of the Cu_{55} and Cu_{923} nanoclusters at 300 K (before melting) and 1200 K (after melting) in the heating and cooling processes.

For the first time, we have presented an analytical expression for the RDF of the confined LJ fluid. We adopted argon as a LJ fluid. Argon is a component of the air, which is an inert gas and has a wide application in industry.[5] It is also utilized in the synthesis of CNTs and CNT bundles of specified characteristic size or chemical functionalization.[16,17] Some previous investigations have proved that the argon can adsorb on the CNTs and CNTs bundles.[18-20] We have also tried to calculate the thermodynamic properties of the confined LJ fluid using the proposed RDF equation. In fact, the investigation of the properties of the confined fluids (such as the RDF) can provide an insight into the many real-world physical and biological phenomena and industrial processes,[1,5] some examples of which are properties of fluids in porous media[21] as in underground petroleum recovery,[22] gas storage,[5] and transfer of ions through biological ion-channels.[23-25]

2. The approach

2.1 The RDF expressions

There are two kinds of the RDFs for the confined LJ fluid into the nanotube; The Ar-Ar RDF and the Ar-C(CNT) RDF. We have calculated the Ar-Ar and Ar-C RDFs of the confined atoms into the (33,0) CNT as a function of reduced separation in the reduced temperature ($T^*=kT/\varepsilon$) and density ($\rho_{mix}{}^*=\rho_{mix}\sigma^3$) ranges from $5.2 \leq T^* \leq 10.4$ (298 K $\leq$ T$\leq$ 600 K) and $1.58 \leq \rho_{mix}{}^* \leq 1.66$ ($160 \leq N_{Ar} \leq 320$) using the MD simulation and then fitted to the following equations using the Sigmaplot software:[26]

$$g_a = s\ \exp\left[-\left(m\ x + n\ \right)^4\right] \qquad x \leq 1 \qquad (1)$$

$$g_b = 1 + (x)^{-4}\exp\left[-\left(a\ \ x + b\ \right)\right]\sin\left[\left(c\,x + d\ \right)\right] + (x)^{-4}\exp\left[-\left(q\ \ x + h\ \right)\right]\cos\left[\left(k\ \ x + l\ \right)\right] \quad x > 1 \qquad (2)$$

where *g* represents the RDF and *a*, *b*, *c*, *d*, *q*, *h*, *k*, *l*, *m*, *n*, and *s* are the adjustable parameters. The details of the fitting procedure and the parameter values of Eqs. (1) and (2) along with the R^2 values for the Ar-Ar and Ar-C RDFs have been presented in Tables S1 and S2 in the supporting information. The Eqs. (1) and (2) are the modifications of our previous expressions for the normal LJ and HFD-like fluids [8,14]. It should be also noted that all of the quantities have been reduced using the Ar-C LJ parameters (Table 1).

The calculated Ar-Ar and Ar-C RDFs of the confined LJ fluid (using the Eqs. (1) and (2)) for the two different confined argon atoms and temperatures have been compared with those of the MD simulation in Figs. 1 and 2, respectively. According to Figs. 1 and 2 and the R^2 values in Tables S1 and S2, there are good agreements between our calculated values and the simulation. It should be also reminded that the Ar-C RDF shows the probability of finding the argon atoms around a reference carbon atom. According to Fig. 2 at N_{Ar}=160, two atomic layers can be distinguished inside the CNT and so, there are two peaks in the Ar-C RDF. It is also shown that there are three peaks (and atomic layers) in the Ar-C RDF at N_{Ar}=320.

2.2 The energy and pressure expressions

We have considered the confined LJ fluid into the CNT as a mixture of the argon and carbon atoms. Therefore, according to the different interactions, the reduced configurational energy of the system, $E^*=E/\varepsilon$ (ε is the well depth of the interaction potential), can be calculated from the following statistical mechanical expression:

$$E^* = \left[2\pi\rho^*_{mix}\int_0^\infty x^2\, U^*(x)\, g^{Ar-Ar}\, dx\right] + \beta_E \left[2\pi\rho^*_{mix}\int_0^\infty x^2\, U^*(x)\, g^{Ar-C}\, dx\right] \tag{3}$$

where $\rho_{mix}{}^* = \rho_{mix}\sigma^3$ is the reduced density of the mixture (σ is the distance at which the intermolecular potential is zero), $x = r/\sigma$ is the reduced intermolecular distance, $U^*(x)$ is the reduced LJ potential, g(r) is the RDF, and β_E is an adjustable constant. According to the two ranges of the RDF equations (Eqs. 1 and 2), the Eq. (3) can be rewritten as:

$$\begin{aligned} E^* = &\left[2\pi\rho^*_{mix}\left(\int_0^1 x^2\, U^*(x)\, g_a^{Ar-Ar}\, dx + \int_1^\infty x^2\, U^*(x)\, g_b^{Ar-Ar}\, dx\right)\right] \\ &+ \beta_E \left[2\pi\rho^*_{mix}\left(\int_0^1 x^2\, U^*(x)\, g_a^{Ar-C}\, dx + \int_1^\infty x^2\, U^*(x)\, g_b^{Ar-C}\, dx\right)\right] \end{aligned} \tag{4}$$

For the LJ fluid confined inside a CNT, the radial and axial forces are different.[27] Therefore, according to the both Ar-Ar and Ar-C interactions, the reduced radial and axial pressures (denoted by P_R and P_L) of the system ($P^* = P\sigma^3/\varepsilon$) can be calculated from the following statistical mechanical expressions:

$$P_R^* = \rho^*_{mix} T^* - \frac{2\pi\rho^{*2}_{mix}}{3}\left[\begin{aligned} &\left(\int_0^1 x^3 \frac{\partial U^*}{\partial x} g_a^{Ar-Ar}\, dx + \int_1^\infty x^3 \frac{\partial U^*}{\partial x} g_b^{Ar-Ar}\, dx\right) \\ &+\beta_R\left(\int_0^1 x^3 \frac{\partial U^*}{\partial x} g_a^{Ar-C}\, dx + \int_1^\infty x^3 \frac{\partial U^*}{\partial x} g_b^{Ar-C}\, dx\right)\end{aligned}\right] \tag{5}$$

$$P_L^* = \rho^*_{mix} T^* - \frac{2\pi\rho^{*2}_{mix}}{3}\left[\begin{aligned} &\left(\int_0^1 x^3 \frac{\partial U^*}{\partial x} g_a^{Ar-Ar}\, dx + \int_1^\infty x^3 \frac{\partial U^*}{\partial x} g_b^{Ar-Ar}\, dx\right) \\ &+\beta_L\left(\int_0^1 x^3 \frac{\partial U^*}{\partial x} g_a^{Ar-C}\, dx + \int_1^\infty x^3 \frac{\partial U^*}{\partial x} g_b^{Ar-C}\, dx\right)\end{aligned}\right] \tag{6}$$

where β_R and β_L are adjustable parameters and $(\partial U^*/\partial x)$ is the first derivative of the reduced interaction potential relative to the reduced intermolecular distance.

2.3 Simulation details

The MD simulations have been performed on the confined argon atoms inside (33,0) CNT with the radius of 1.29 nm and the length of 4.24 nm from room temperature to 600 K and for the confined 160 to 320 argon atoms. During the simulation, one (33,0) CNT was immersed in an equilibrated periodic LJ fluid reservoir containing 8000 argon atoms.

Without any filling, an initial optimization at the pressure of 1 atm and the temperature of 300 K was performed and the argon atoms were allowed to fill into the nanopore from the bulk outer fluid (Fig. 3). After completing the filing process (320 confined atoms after about 5 ns), the system was equilibrated for 5 ns. We also ran simulations by diminishing the confined atoms into the CNT from 320 to 160 (by 20 atoms) and then we equilibrated the system for 5 ns again.

The MD simulations were carried out in canonical ensemble (*NVT*). The equations of motion were integrated using Verlet leapfrog algorithm with a time step of 0.001 ps. In these simulations, we have used Nose-Hoover thermostat algorithm[28,29] with DLPOLY 4.03 package.[30] The relaxation time for thermostat is 0.1 fs. The periodic boundary conditions were applied only in the axial direction of the CNT. All interatomic interactions between the atoms in the simulation box have been calculated within the cutoff distance 15 Å. The simulations were carried out for 5 ns of equilibration followed by production time of 2 ns for the calculated properties (The details of the choosing of 5 ns as the equilibration time have been presented in the supporting information). The Argon-Argon interaction energy was modeled using the Lennard-Jones (12,6) potential.[31] In these simulations, the CNTs have been kept in fixed position. For the intermolecular interactions between Argon and CNT, we have used Lennard- Jones potential utilizing the geometric mean for ε and the arithmetic mean for σ.[32] Table 1 shows the different LJ interactions used in this work.

3. Results and discussion

3.1 The confinement effect

We have compared the Ar-Ar RDF of the normal (non-confined) fluid with the Ar-Ar RDFs of the fluid confined into the (33,0) and (19,0) CNTs in Fig. 4. According to this figure, the RDF, or g(r) =ρ(r)/ρ, of a normal LJ fluid tends toward zero as the reduced distance x(=r/σ) goes to zero, since additional particles cannot occupy the same location as the reference particle. It is also shown at large distance, the influence of the reference particle is zero, and g(r) must approach unity (which means that the local density (ρ(r)) is equal to the macroscopic density (ρ). It is also illustrated at intermediate separation, $\rho(r)$ may be less than or exceed ρ, depending on whether the distance r corresponds to the repulsion or attraction between the particles.[7]

According to Fig. 4, the Ar-Ar RDF of the confined fluid into the (33,0) CNT has three differences with that of the normal fluid. First, the RDF peaks are higher for the confined fluid. This means that there is more probability of finding other particles around a reference atom in a confined fluid than the normal fluid. Second, there are less peaks and oscillations (almost three peaks) in the RDF of the confined fluid than the normal one. This means that there are less layers of the neighbor particles around the reference atom in the confined fluid than the normal one. Third, the RDF does not approach unity at large distances but approaches to a number which is greater than unity (here is about 4). The reason of all of these differences is called the confinement effect.[4] In the other words, the density of the argon atoms in the atomic layers (in the confinement state) is evidently higher than the density of the normal fluid due to the layered structure inside the CNT. It is also shown in Fig. 4 that there are two atomic layers inside the (19,0) CNT in which the first atomic layer locates at the center of the tube. It is also shown that the Ar-Ar RDF peaks are higher in the (19,0) CNT which is due to the stronger confinement effect in the smaller CNT than the bigger nanotube.

3.2 Calculation of configurational energy

We have considered the confined LJ fluid into the CNT as a mixture of the argon and carbon atoms. In Eq. (4), the β_E is an adjustable parameter which its value for a homogeneous mixture is 2. It should be noted that our system (confined Ar atoms into the CNT) is a heterogeneous mixture of argon and carbon atoms and so, the value of the parameter β_E should be investigated.

We have determined the values of the parameter β_E at different temperatures and densities (different argon atoms) by comparison between the calculated energy values from Eq. (4) and the MD simulated data and presented in Fig. 5. According to this figure, the β_E values show almost the same trend at different temperatures and their values are between 1 to 5. The β_E values increase sharply with increasing the confined argon atoms in the CNT until the N_{Ar}=240 and then become almost constant. It is also shown that the β_E values increase with increasing the temperature.

Suppose a homogeneous mixture of argon and carbon atoms. For this mixture, increasing the temperature or density will change the Ar-Ar and Ar-C interactions in the mixture identically and so the both terms in the Eq. (3) changes identically and the β_E will be constant (which is 2). But for our heterogeneous system, by increasing the temperature or density, the significance of the second term increases than the first term in Eq. (3). In the other words, the interactions and collisions between the confines atoms and the CNT wall increase by increasing the density and temperature. It is also surprising that the β_E is almost equal to 2 at high densities for 300 to 400 K which is equal to the value for the homogeneous mixture.

We have also compared the simulated values of the configurational energy and our calculated energy values for the confined argon atoms into the (33,0) CNT using the Eq. (4) and the RDF values calculated from Eqs (1) and (2) in Fig. 6. According to this figure, there are very good agreements between our calculated and the simulated values.

3.3 Radial and axial pressures

For the LJ fluid confined inside a CNT, the radial and axial forces are different.[27] Therefore, we have two kind of pressure for the system; radial pressure and axial pressure. According to Eqs. (5) and (6), it may be very difficult or impossible to introduce the interaction potential and RDF in the radial and axial directions. Instead, we have used alternative method. It is obvious that the both Ar-Ar and Ar-CNT interactions are responsible for the radial or axial pressures. Therefore, we have tried to know what combination of the Ar-Ar and Ar-C terms in Eqs. (5) and (6) is responsible for the radial pressure or axial pressure. In the other words, we have considered the same interaction LJ potential and the same RDF equations (Eqs. 1 and 2) but the different adjustable parameters (β_R and β_L) for the both radial and axial pressure equations. Such as the energy calculation, we have also considered the confined LJ fluid into the CNT as a heterogeneous mixture of the argon and carbon atoms.

We have determined the values of the parameters β_R and β_L at different temperatures and densities (different argon atoms) by comparison between the calculated pressure values from Eqs. (5) and (6) and the MD simulated data and presented in Fig. 7. According to this figure, the β_R and β_L values show almost the same trend at different temperatures and their values are between 0 to 2. It is shown until the N_{Ar}= 300 that the both β_R and β_L parameters oscillate around average values of 0.95 and 0.92, respectively. It means that the second parenthesis in Eqs. (5) and (6) (i.e. the Ar-wall interaction) is a bit more significant than the first parenthesis in the radial pressure. After the N_{Ar}= 300, the both β_R and β_L parameters increase sharply with the confined atoms as expected. The different trends of the both β_R and β_L parameters relative to the β_E parameter can be due to the fact that the LJ fluid inside the nanotube is an anisotropic system for which the pressure is a tensor.

We have also compared the simulated values of the radial and axial pressures and our calculated pressure values for the confined argon atoms in the (33,0) CNT using the Eqs. (5) and (6) and the RDF values calculated from Eqs. (1) and (2) in Fig. 8. According to this figure, there are very good agreements between our calculated and simulated pressure values. These good agreements between our simulated and calculated values verify the new expressions proposed for the RDF of the confined LJ fluid.

4. Conclusion

We have calculated the Ar-Ar and Ar-C RDFs of the confined argon atoms into the (33,0) CNT as a function of reduced separation in the reduced temperature and density ranges from $5.2 \leq T^* \leq 10.4$ and $1.58 \leq \rho_{mix}{}^* \leq 1.66$ using the MD simulation. Then, we have fitted the obtained RDF values to new analytical expressions whose the R^2 values of the adjustable constants (Tables S1 and S2) show good agreements with the simulated values.

We have considered the confined LJ fluid into the CNT as a heterogeneous mixture of the argon and carbon atoms and calculated the reduced configurational energy and radial and axial pressures of the system from the statistical mechanical expressions. In order to get the good agreement between the calculated and simulated values of the thermodynamic properties, we have introduced the adjustable parameters β_E, β_R, and β_L for the configurational energy, radial pressure, and axial pressure, respectively. Our energy results showed that the β_E values increase with the confined argon atoms and the temperature which can be due to the more significance of the second term than the first term in Eq. (3).

Our pressure results indicated that the β_R and β_L values show almost the same trend at different temperatures and they oscillate around average values of 0.95 and 0.92, respectively. The different trends of the both β_R and β_L parameters relative to the β_E parameter can be due to the fact that the LJ fluid inside the nanotube is an anisotropic system for which the pressure is a tensor. We have also calculated the configurational energy, radaial and axial pressures using the new RDF expressions for the confined LJ fluid in very good agreements with the simulated values.

For the first time, we have presented the analytical expressions for the RDF of the confined LJ fluid (Eqs. 1 and 2). In fact, the investigation of the properties of the confined fluids (such as the RDF) can provide an insight into the many real-world physical and biological phenomena and industrial processes, some examples of which are properties of fluids in porous media as in underground petroleum recovery, gas storage, and transfer of ions through biological ion-channels.

Keywords: Radial distribution function; Confined Lennard-Jones fluid; Carbon nanotube; Radial and axial pressure; Configurational energy.

References

1 G. A. mansoori and S. A. Rice, *Adv. Chem. Phys.*, 2014, **156**, 1.

2 H. F. Ye, H. W. Zhang, Y. G. Zheng and Z. Q. Zhang, *Microfluid. Nanofluid.*, 2011, **10**,1359.

3 H. W. Zhang, H. F. Ye, Y. G. Zheng and Z. Q. Zhang, *Microfluid. Nanofluid.*, 2011, **10**, 403.

4 H. Ye, Z. Zhang, Y. Zheng, H. Zhang, Z. Chen and Z. Zong, *Int. J. Comput. Mater. Sci. Eng.*, 2014, **3**, 1450018.

5 C. K. Das and J. K. Singh, *Theor. Chem. Acc.* 2013, **132**, 1351.

6 H. Akbarzadeh, M. Abbaspour, S. Salemi and M. Abroodi, *Phys. Chem. Chem. Phys.*, 2015, **17**, 12747.

7 D.A. McQaarrie, *Statistical Mechanics*, Harper and Row, New York, 1975.

8 A. Morsali, E. K. Goharshadi, G. A. Mansoori and M. Abbaspour, *Chem. Phys*. 2005, **310**, 11.

9 T. L. Hill, *Statistical Mechanics*, McGraw-Hill, New York, 1956.

10 J. M. Haile and G.A. Mansoori, *Molecular-Based Study of Fluids*, American Chemical Society, Washington D.C., 1983.

11 E. Matteoli and G.A. Mansoori, *Fluctuation Theory of Mixtures*, Taylor & Francis Publ. Co., New York, NY, 1990.

12 E. Matteoli and G.A. Mansoori, *J. Chem. Phys.,* 1995, **103**, 4672.

13 M. Abbaspour and A. Keyvanloo, *J. Mol. Liq.,* 2013, **177**, 1.

14 M. Abbaspour and M. N. Jorabchi, , *J. Mol. Liq.,* 2014, **195**, 175.

15 G. Ori, F. Villemota, L. Viauc, A. Viouxa and B. Coasne, *Mol. Phys.*, 2014, **112**, 1350.

16 S. Farhat, M. L. de La Chapelle, A. Loiseau, C. D. Scott, S. Lefrant, C. Journet and P. Bernier, *J. Chem. Phys*. 2001, **115**, 6752.

17 D. Q. Yang, J. F. Rochette and E. Sacher, *Langmuir*, 2005, **21**, 8539.

18 M. Bienfait, P. Zeppenfeld, N. Dupont-Pavlovsky, J. P. Palmari, M. R. Johnson, T. Wilson, M. De Pies and O. E. Vilches, *Phys. Rev. Lett*. 2003, **91**, 035503.

19 S. Rols, M. R. Johnson, P. Zeppenfeld, M. Bienfait, O. E. Vilches and J. Schneble, *Phys. Rev. B*, 2005, **71**, 155411.

20 Y. C. Liu, J. D. Moore, T. J. Roussel and K. E. Gubbins, *Phys. Chem. Chem. Phys.*, 2010, **12**, 6632.

21 F. Štěpánek, M. Šoóš and P. Rajniak, *Colloid Surf. A*, 2007, **300**, 11.

22 B. Henrich, C. Cupelli, M. Santer and M. Moseler, *New J. Phys*. 2008, **10**, 113022.

23 W. A. Catterall, *Science*, 1988, **242**, 50.

24 V. Krishnamurthy and B. Cornell, *Protoplasma*, 2012, **249**, 3.

25 T. A. van der Straaten, J. Tang and R. S. Eisenberg RS, *J. Comp. Electronics*, 2002, **1**, 335.

26 Sigmaplot, Version 10.0 (2006), Systat Software, San Jose, CA.

27 M. Sadeghi, G. A. Parsafar, *J. Phys. Chem. B*, 2012, **116**, 4943.

28 S. Nose, *J. Phys.: Condens. Matter.*, 1990, **2**, 115.

29 W. G. Hoover, *Phys. Rev. A*, 1985, **31**, 1695.

30 W. Smith and I. T. Todorov, *Mol. Simul.*, 2006, **32**, 935.

31 J. O. Hirschfelder, C. F Curtiss and R. B. Bird, *Molecular Theory of Gases and Liquids*, Wiley, New York, 1954.

32 D. D. Do, H. D. Do and K. Kaneko, *Langmuir* 2004, **20**, 7623.

Figure captions

Fig. 1. Comparison between our calculated Ar-Ar RDFs of the confined LJ fluid (using the Eqs. (1) and (2)) and those of the MD simulation at different states.

Fig. 2. Comparison between our calculated Ar-C(CNT) RDFs of the confined LJ fluid and those of the MD simulation at different states.

Fig. 3. The Snapshot of the nanotube immersed in 8000 argon atoms at 300K.

Fig. 4. Comparison between the Ar-Ar RDFs of the normal (non-confined) and the confined LJ fluids into the (33,0) and (19,0) CNTs.

Fig. 5. The β_E values at different temperatures and densities (different argon atoms).

Fig. 6. Comparison between the simulated values (points) of the configurational energy and our calculated values (solid lines) using the Eq. (4) and the RDF equations (Eqs. 1 and 2).

Fig. 7. The β_R and $\beta_L$values at different temperatures and densities (different argon atoms).

Fig. 8. Comparison between the simulated values (points) of the radial and axial pressures and our calculated values (solid lines) using the Eqs. (5) and (6) and the RDF equations (Eqs. 1 and 2). The symbols have the same meaning of Fig. 6.

Table 1. The values of LJ parameters for the different interactions.[30,31]

Interaction	σ (Å)	ε/k (K)
Ar-Ar	3.4050	119.80
Ar-C(CNT)	3.4025	57.67

Fig. 1

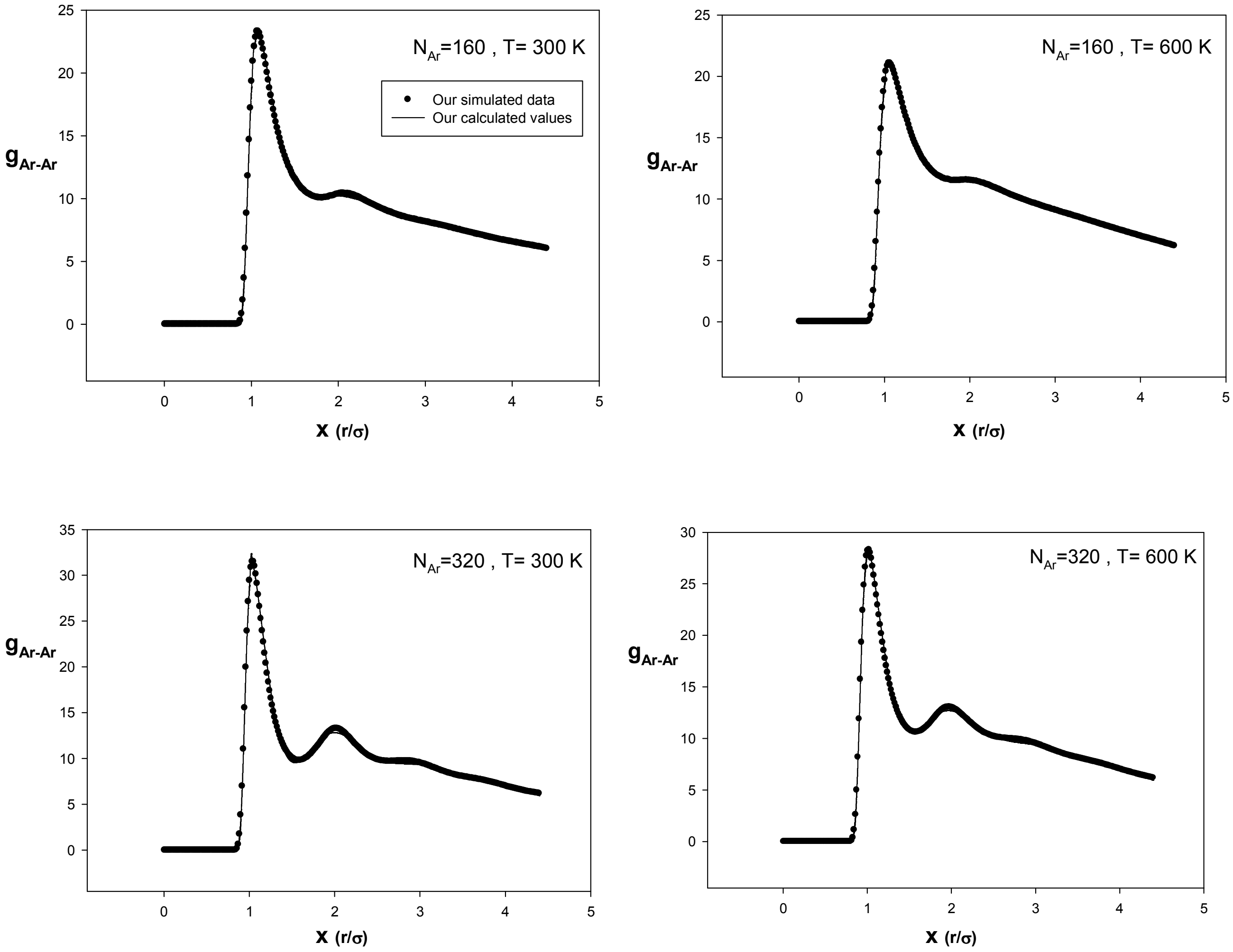
N$_{Ar}$=160 , T= 300 K
Our simulated data
Our calculated values
$g_{Ar\text{-}Ar}$
0
5
10
15
20
25
0
1
2
3
4
5
x (r/σ)
N$_{Ar}$=160 , T= 600 K
$g_{Ar\text{-}Ar}$
0
5
10
15
20
25
0
1
2
3
4
5
x (r/σ)
N$_{Ar}$=320 , T= 300 K
$g_{Ar\text{-}Ar}$
0
5
10
15
20
25
30
35
0
1
2
3
4
5
x (r/σ)
N$_{Ar}$=320 , T= 600 K
$g_{Ar\text{-}Ar}$
0
5
10
15
20
25
30
0
1
2
3
4
5
x (r/σ)

Fig. 2

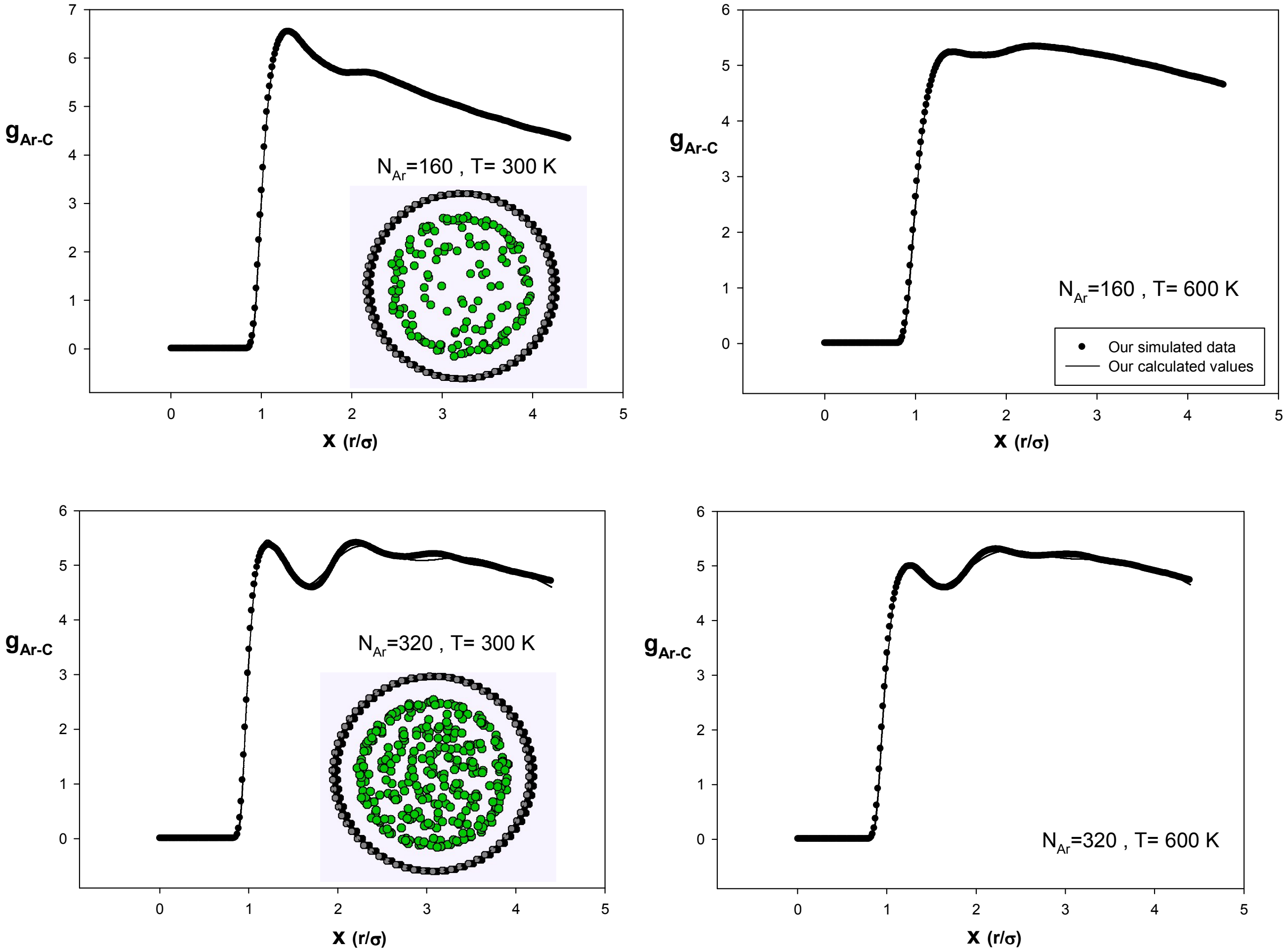
g_{Ar-C}
N_{Ar}=160 , T= 300 K
N_{Ar}=160 , T= 600 K
● Our simulated data
— Our calculated values
N_{Ar}=320 , T= 300 K
N_{Ar}=320 , T= 600 K
X (r/σ)
0
1
2
3
4
5
6
7

Fig. 3

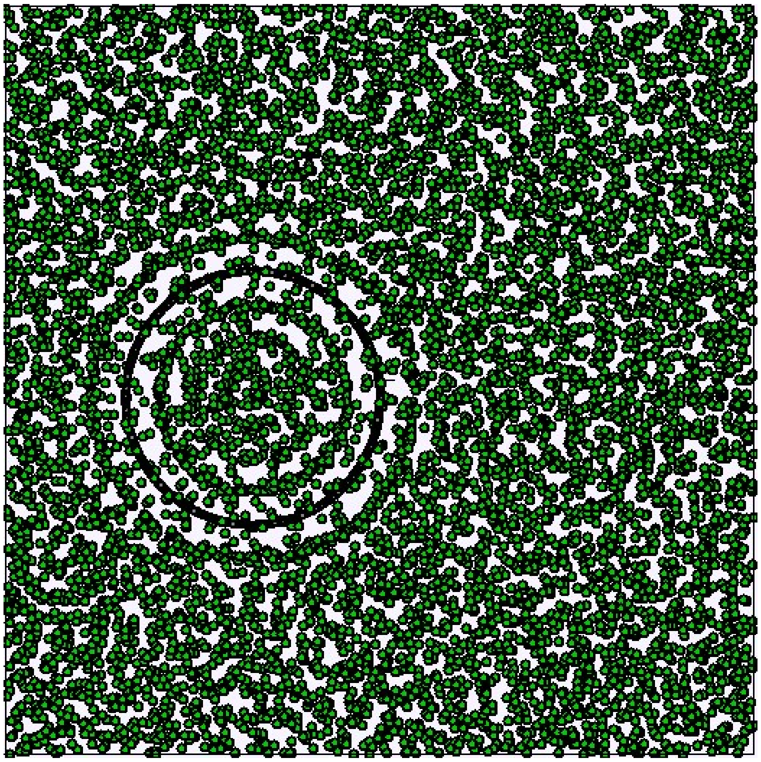

Fig. 4

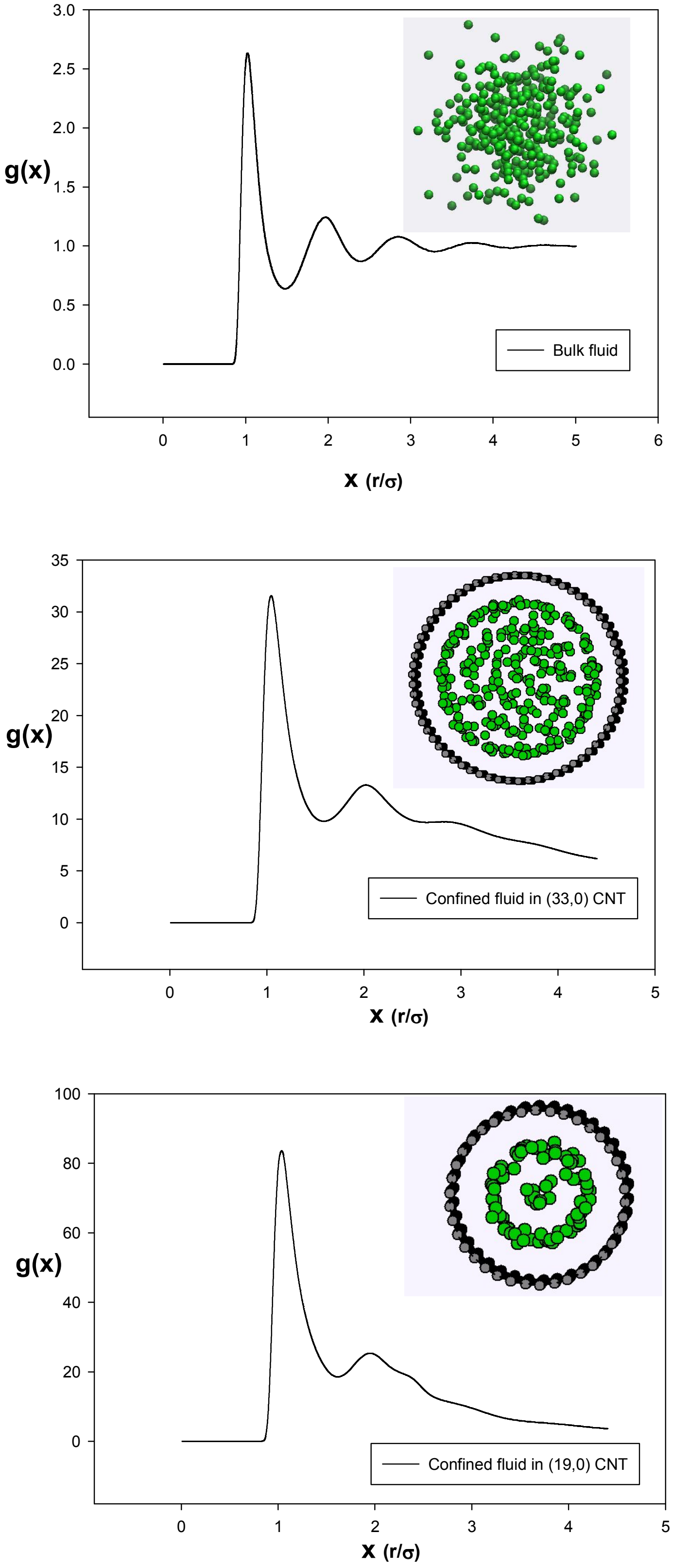
3.0
2.5
2.0
g(x)
1.5
1.0
0.5
0.0
0
1
2
3
4
5
6
X (r/σ)
Bulk fluid
35
30
25
20
g(x)
15
10
5
0
0
1
2
3
4
5
X (r/σ)
Confined fluid in (33,0) CNT
100
80
60
g(x)
40
20
0
0
1
2
3
4
5
X (r/σ)
Confined fluid in (19,0) CNT

Fig. 5

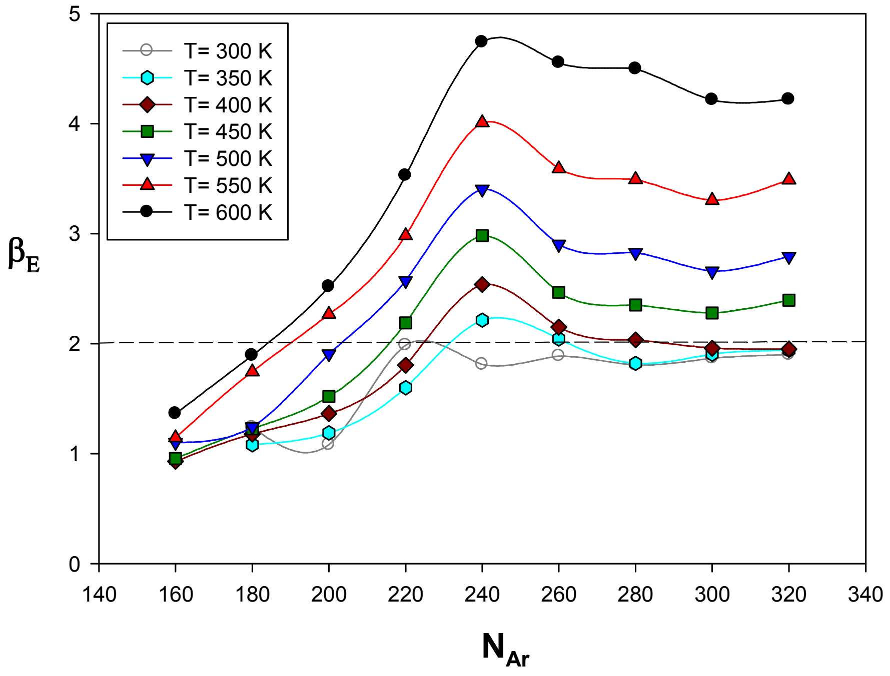

T= 300 K
T= 350 K
T= 400 K
T= 450 K
T= 500 K
T= 550 K
T= 600 K
β_E
0
1
2
3
4
5
140
160
180
200
220
240
260
280
300
320
340
N_{Ar}

Fig. 6

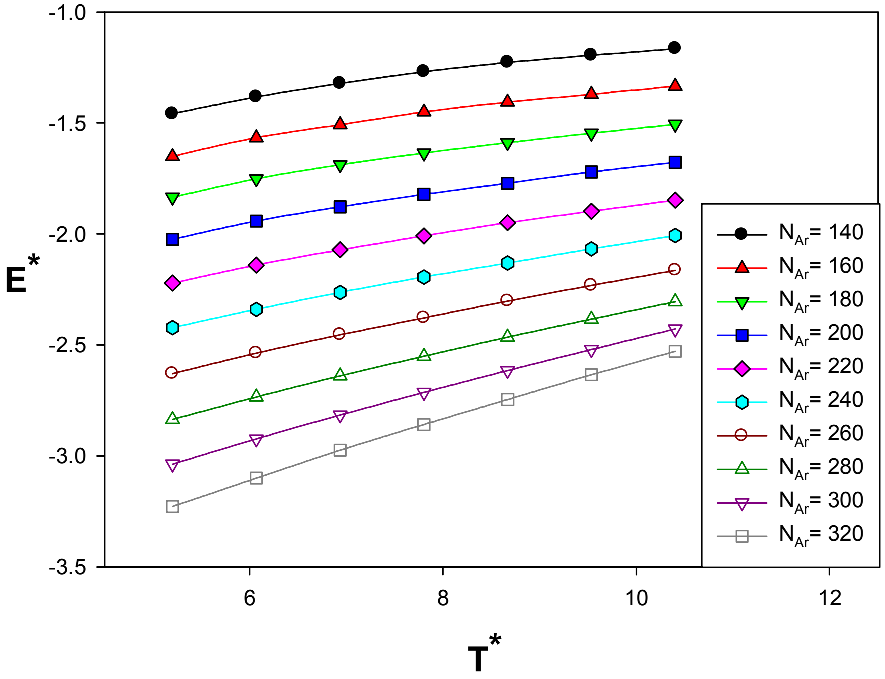
-1.0
-1.5
-2.0
-2.5
-3.0
-3.5
E^*
6
8
10
12
T^*
N_{Ar}= 140
N_{Ar}= 160
N_{Ar}= 180
N_{Ar}= 200
N_{Ar}= 220
N_{Ar}= 240
N_{Ar}= 260
N_{Ar}= 280
N_{Ar}= 300
N_{Ar}= 320

Fig. 7

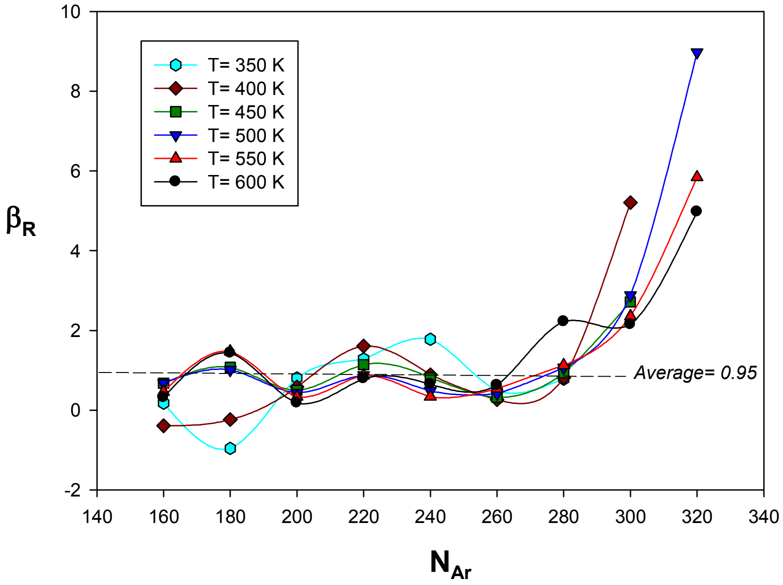
10
8
6
4
2
0
-2
140
160
180
200
220
240
260
280
300
320
340
β_R
N_{Ar}
T= 350 K
T= 400 K
T= 450 K
T= 500 K
T= 550 K
T= 600 K
Average= 0.95

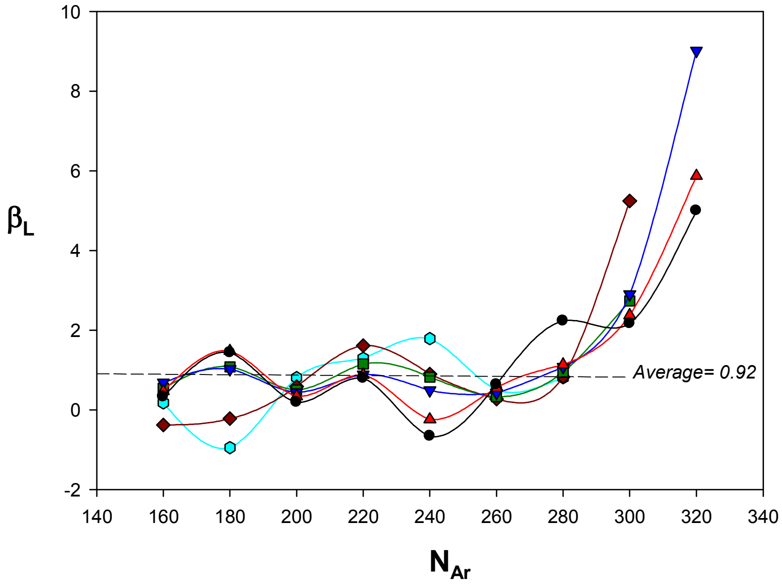
10
8
6
4
2
0
-2
140
160
180
200
220
240
260
280
300
320
340
β_L
N_{Ar}
Average= 0.92

Fig. 8

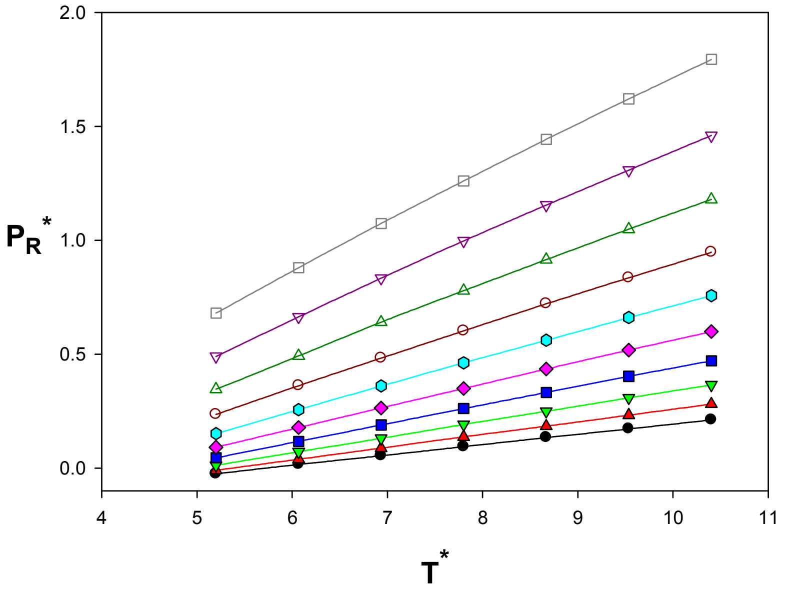

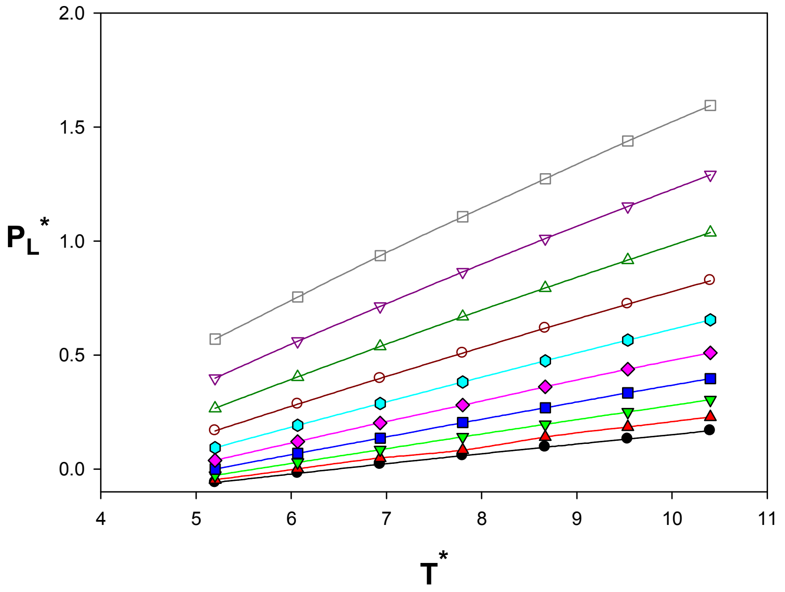

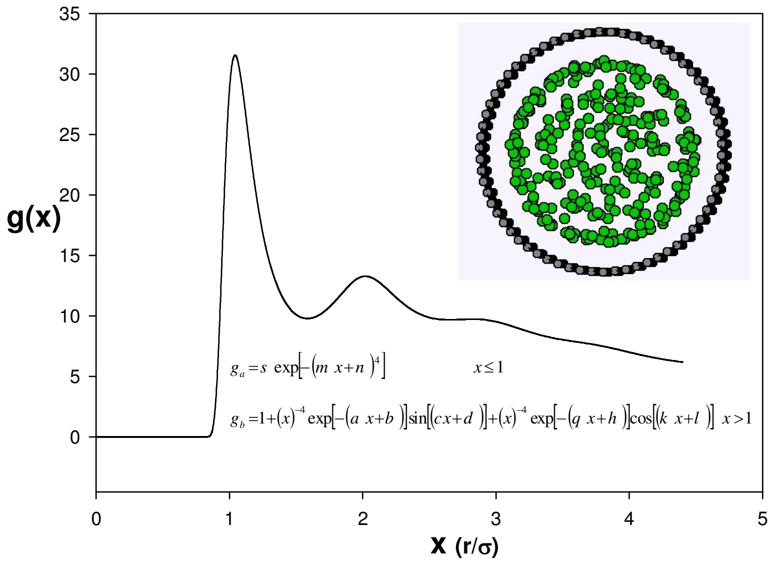

A new and accurate expression for the RDF of the confined LJ fluid into carbon nanotube has been obtained.